A STABLE AND ACCURATE BUTTERFLY SPARSE FOURIER TRANSFORM

STEFAN KUNIS[†] AND INES MELZER[‡]

Abstract. Recently, the butterfly approximation scheme has been proposed for computing Fourier transforms with sparse and smooth sampling in frequency and spatial domain. We present a rigorous error analysis which shows how the local expansion degree depends on the target accuracy and the nonharmonic bandwidth. Moreover, we show that the original scheme becomes numerically unstable if a large local expansion degree is used. This problem is removed by representing all approximations in a Lagrange type basis instead of the previously used monomial basis. All theoretical results are illustrated by numerical experiments.

Key words and phrases : trigonometric approximation, nonharmonic Fourier series, fast Fourier transform.

2010 AMS Mathematics Subject Classification : 65T40, 65T50, 42A15.

1. Introduction. The fast Fourier transform (FFT) [4, 8] belongs to the algorithms with large impact on science and engineering. Shortcomings are the need for equispaced sampling and the fact that sparsity, as used in many recent approaches to tackle large scale and high dimensional problems, is not reflected in reduced computational costs.

The development of nonequispaced FFTs is well understood, see e.g. [10] and references therein, and the common concept in such schemes is to trade exactness for efficiency; instead of precise computations up to machine precision, the proposed methods guarantee a given target accuracy. In its most general form, given a space dimension $d \in \mathbb{N}$, a nonharmonic bandwidth $N = 2^L$, $L \in \mathbb{N}$, a set of frequencies $\widetilde{T} = \{\boldsymbol{\xi}_k \in [0,N]^d : k = 1,\dots,M_2\}$, a set of Fourier coefficients $\hat{u}_k \in \mathbb{C}$, $k = 1,\dots,M_2$, and a set of evaluation nodes $\widetilde{X} = \{\boldsymbol{x}_j \in [0,N]^d : j = 1,\dots,M_1\}$, we aim to compute the sums

$$u_j := u(\boldsymbol{x}_j) = \sum_{k=1}^{M_2} \hat{u}_k \mathrm{e}^{2\pi \mathrm{i} \boldsymbol{\xi}_k \boldsymbol{x}_j / N}, \quad j = 1,\dots,M_1. \tag{1.1}$$

While the naive computation takes $\mathcal{O}(M_1 M_2)$ floating point operations, the FFT for nonequispaced data in space and frequency domain [6] or type-3 nonuniform FFT [9] reduce this to $\mathcal{O}(N^d \log N + |\log \varepsilon|^d (M_1 + M_2))$, where $\varepsilon > 0$ denotes the target accuracy.

Yet another analysis-based fast algorithm is the butterfly approximation scheme, which can be traced back at least to [12] and has found a series of recent applications in [18, 13, 16, 3]. Moreover it is well known that certain blocks of the discrete Fourier transform are approximately of low rank [5], which has lead to the butterfly sparse Fourier transforms [1, 17]. Hence, the sums (1.1) with $d \geq 2$, $M_1 = M_2 = \mathcal{O}(N^{d-1})$, and well distributed sampling sets $\widetilde{T}, \widetilde{X}$ on smooth $d-1$ dimensional manifolds, can be computed in $\mathcal{O}(N^{d-1} \log N p^{d+1})$ floating point operations, where $p \in \mathbb{N}$ denotes the local expansion degree.

In this paper, we follow [17] and present a rigorous error analysis which shows how the local expansion degree depends on the target accuracy and the nonharmonic

[†]University Osnabrück, Institute of Mathematics, and Helmholtz Zentrum München, Institute for Biomathematics and Biometry, stefan.kunis@math.uos.de

[‡]University Osnabrück, Institute of Mathematics, ines.melzer@uos.de

bandwidth. After introducing the necessary notation and modifying the original approach slightly, we prove in Theorem 2.6 an error estimate given a local admissibility condition is fulfilled. The combination of the local approximation is done via the butterfly scheme in Section 3 and we prove how the error propagates through the different levels of the method in Theorem 3.1 - this also allows for a complexity estimate. Moreover, we show that the original scheme becomes numerically unstable if a large local expansion degree is used and remove this problem by representing all approximations in a Lagrange type basis instead of the previously used monomial basis, cf. Section 2.4. All theoretical results are illustrated by numerical experiments and we finally conclude our findings in Section 5.

2. Prerequisites and local approximation. Let the numbers $p, N \in \mathbb{N}$, $p \geq 2$, be fixed and let the Chebyshev polynomials of the first kind $T_p : [-1,1] \to \mathbb{R}$, $T_p(t) = \cos(p \arccos t)$, be given. The zeros of the p-th Chebyshev polynomial are given by

$$t_j = \cos \frac{2j+1}{2p}\pi, \quad j = 0, \dots, p-1, \tag{2.1}$$

and we define the corresponding Lagrange polynomials $L_k : \mathbb{R} \to \mathbb{R}$ by

$$L_k(t) = \prod_{\substack{j=0 \\ j \neq k}}^{p-1} \frac{t - t_j}{t_k - t_j}, \quad k = 0, \dots, p-1. \tag{2.2}$$

For subsequent use, we collect the following auxiliary estimates which are either standard or can be found e.g. as exercises in [14].

LEMMA 2.1. *For $p \in \mathbb{N}$, $p \geq 3$, and $x \in \mathbb{R}$, $|x| \leq \frac{2\pi}{p-1}$, we have*

$$\cos \frac{2\pi}{p-1} \leq \cos x, \tag{2.3}$$

$$1 - \frac{x^2}{2} \leq \cos x, \tag{2.4}$$

$$\left(1 - \cos \frac{2\pi}{p-1}\right) \frac{(p-1)^2}{2\pi^2} \leq \frac{2(1-\cos x)}{x^2}, \tag{2.5}$$

$$\frac{16}{\pi^4} \leq \left(\frac{2(1-\cos x)}{x^2}\right)^{\frac{2\pi}{x}} \overset{x \to 0}{\longrightarrow} 1. \tag{2.6}$$

Proof. The first estimate follows since the cosine is decreasing in $[0, \frac{2\pi}{p-1}] \subset [0, \pi]$ and even. Integrating $\cos x \leq 1$ twice yields the second claim.

The relations $x \leq \tan x$ for $x \in [0, \frac{\pi}{2})$ and $\cos x \leq 0$, $\sin x \geq 0$, $x \geq 0$ for $x \in [\frac{\pi}{2}, \pi]$, yield $x \cos x - \sin x \leq 0$ and by integration

$$x \sin x - 2(1 - \cos x) \leq 0, \qquad x \in [0, \pi].$$

Dividing by $x^3/2$ this yields $f'(x) \leq 0$ for the even function $f(x) = \frac{2(1-\cos x)}{x^2}$ and thus $f(x) \geq f\left(\frac{2\pi}{p-1}\right)$, $|x| \leq \frac{2\pi}{p-1}$, which is the third assertion.

Considering $x \in [-\pi, 0)$, we have $0 < f(x) \leq 1$ and together with L'Hospitals rule

$$(f(x))^{\frac{2\pi}{x}} \geq 1, \ x \in [-\pi, 0), \quad \text{and} \quad \frac{2\pi}{x} \log f(x) \to 0, \ x \to 0.$$

Setting $g(x) = \frac{x}{2\pi}\log\frac{16}{\pi^4}$ and $h(x) = \log f(x)$ yields $g(0) = h(0)$, $g(\pi) = h(\pi)$, and

$$h''(x) = -\frac{1}{1-\cos x} + \frac{2}{x^2} \le 0, \quad x \in [0,\pi].$$

Hence, the function h is concave and we obtain $h(x) \ge g(x)$. Since g is decreasing, this yields the assertion $\frac{2\pi}{x}h(x) \ge \log\frac{16}{\pi^4}$. □

LEMMA 2.2. *For $p \in \mathbb{N}$, $p \ge 3$, the Chebyshev roots* (2.1) *and the corresponding Lagrange polynomials* (2.2) *obey*

$$\prod_{\substack{k=0\\k\neq n}}^{p-1} |t_k| = \frac{p}{2^{p-1}} \quad \text{if } p = 2n+1,\ n \in \mathbb{N}, \tag{2.7}$$

$$\max_{x\in[-1,1]} \sum_{s=0}^{p-1} (L_s(x))^2 \le 2, \tag{2.8}$$

$$\max_{x\in[-1,1]} \sum_{s=0}^{p-1} |L_s(x)| \le 1 + \frac{2}{\pi}\log p, \tag{2.9}$$

$$\max_{x\in[-3,3]} |L_s(x))| \le \frac{34^{\frac{p}{2}}}{4p}. \tag{2.10}$$

Proof. Let $p = 2n+1$, $n \in \mathbb{N}$, then $t_n = 0$ and $L_n(0) = 1$. Moreover, we have $T_p'(0) = pU_{p-1}(0) = p$, where $U_{p-1}(\cos\theta) = \frac{\sin p\theta}{\sin\theta}$ denotes the Chebyshev polynomial of second kind. Via the representation

$$L_s(x) = \frac{T_p(x)}{(x-t_s)T_p'(t_s)} \tag{2.11}$$

and $T_p(x) = 2^{p-1}\prod_{j=0}^{p-1}(x-t_j)$ this yields for $x = 0$ the first assertion.

The Gauss-Chebyshev quadrature yields the discrete orthogonality

$$\sum_{s=0}^{p-1} T_k(t_s)T_l(t_s) = \begin{cases} 0 & \text{for } k \neq l, \\ p & \text{for } k = l = 0, \\ \frac{p}{2} & \text{for } k = l \neq 0, \end{cases}$$

and since $L_s(t_j) = \delta_{s,j}$ also the expansion of the Lagrange polynomials

$$L_s(x) = \frac{2}{p}\sum_{j=0}^{p-1}{}' T_j(t_s)T_j(x) := \frac{1}{p}T_0(t_s)T_0(x) + \frac{2}{p}\sum_{j=1}^{p-1} T_j(t_s)T_j(x),$$

where the prime indicates that the first summand is weighted by $\frac{1}{2}$. Hence, we have

$$\begin{aligned}\sum_{s=0}^{p-1}(L_s(x))^2 &= \sum_{s=0}^{p-1}\frac{4}{p^2}\left(\sum_{k=0}^{p-1}{}' T_k(t_s)T_k(x)\right)\left(\sum_{l=0}^{p-1}{}' T_l(t_s)T_l(x)\right) \\ &= \frac{4}{p^2}\sum_{k=0}^{p-1}{}'\sum_{l=0}^{p-1}{}' T_k(x)T_l(x)\sum_{s=0}^{p-1} T_k(t_s)T_l(t_s)\end{aligned}$$

and since $|T_k(x)| \le 1$ for $x \in [-1,1]$ the second claim by

$$\le \frac{4}{p^2}\left(\frac{1}{4}p + (p-1)\frac{p}{2}\right) \le 2.$$

The third estimate is the classical Lebesgue constant, cf. [14, Thm. 1.2].

Finally, we note that (2.8) implies $|L_s(x))| \le \sqrt{2}$ for $|x| \le 1$ and it remains to show the bound for $|x| \in [1,3]$. Since L_s is a polynomial and has all its zeros inside $[-1,1]$, it attains its extrema at $x = \pm 3$. Using once more (2.11), the explicit formula

$$T_k(x) = \frac{(x+\sqrt{x^2-1})^k + (x-\sqrt{x^2-1})^k}{2}, \quad |x| \ge 1,$$

the simple bound $(\pm 3 - t_s)^2 \ge 4$, and

$$(U_{p-1}(t_s))^2 = \frac{\sin^2\left(\frac{2s+1}{2}\pi\right)}{\sin^2\left(\frac{2s+1}{2p}\pi\right)} \ge \sin^2\left(\frac{2s+1}{2}\pi\right) = (-1)^{2s} = 1, \quad s = 0,\dots,p-1,$$

we end at the last assertion. □

2.1. Interpolation operators. We call $A := [a,b]$, $a < b$, box and denote its width and its center by $w^A := \operatorname{diam} A = b - a$ and $c^A := \frac{a+b}{2}$, respectively. Further, we define in $\left[-\frac{1}{2}, \frac{1}{2}\right]$ the vector of the normalised Chebyshev nodes and the vector of the equispaced nodes by

$$\boldsymbol{\alpha} = (\alpha_j)_{j=0}^{p-1},\ \alpha_j = \frac{1}{2}t_j, \quad \boldsymbol{\beta} = (\beta_j)_{j=0}^{p-1},\ \beta_j = \frac{1}{2} - \frac{j}{p-1}.$$

For a box $B \subset \mathbb{R}$ we define the linear space of all finite expansions of exponential functions

$$\Pi_B(A) := \left\{ g : A \to \mathbb{C} : g(x) = \sum_{j=1}^{K} \hat{g}_j \mathrm{e}^{2\pi \mathrm{i} \xi_j x/N},\ K \in \mathbb{N},\ \hat{g}_j \in \mathbb{C},\ \xi_j \in B \right\}$$

and its subspace with p equispaced frequencies $\xi_j^B := c^B + \beta_j w^B$,

$$\Pi_B^p(A) := \left\{ g : A \to \mathbb{C} : g(x) = \sum_{j=0}^{p-1} \hat{g}_j^{AB} \mathrm{e}^{2\pi \mathrm{i} x \xi_j^B/N},\ \hat{g}_j \in \mathbb{C} \right\}. \tag{2.12}$$

Let $C(A)$ denote the space of continuous functions on A and define the trigonometric interpolation operator

$$\mathcal{J}_p^{AB} : C(A) \to \Pi_B^p(A), \quad g \mapsto \mathcal{J}_p^{AB} g = \sum_{s=0}^{p-1} \hat{g}_s^{AB} \mathrm{e}^{2\pi \mathrm{i} x \xi_s^B/N}, \tag{2.13}$$

such that in the (shifted and dilated) Chebyshev nodes

$$x_r^A := c^A + \alpha_r w^A \tag{2.14}$$

the interpolation condition $\mathcal{J}_p^{AB} g(x_r^A) = g(x_r^A)$ for $r = 0,\dots,p-1$ holds true.

In order to analyse this interpolation operator, we need a small detour on interpolation by polynomials

$$\widetilde{\Pi}_{p-1}(\mathbb{C}) := \left\{ q : \mathbb{C} \to \mathbb{C} : q(z) = \sum_{j=0}^{p-1} c_j z^j : c_j \in \mathbb{C} \right\}$$

in the complex plane. Let the mapping $z : A \to \mathbb{C}$,

$$z(x) := \mathrm{e}^{-2\pi \mathrm{i} x \frac{w^B}{(p-1)N}}, \tag{2.15}$$

and nodes $z_j^{AB} := z(x_j^A)$ on the arc $\Gamma_p^{AB} := z(A)$ be given. Under the so-called admissibility condition $w^A w^B \leq N$ and for $p \geq 2$, the nodes are distinct and we define the Lagrange polynomials $\widetilde{L}_k^{AB} : \mathbb{C} \to \mathbb{C}$ and the interpolation operator $\mathcal{I}_p^{AB} : C(\Gamma_p^{AB}) \to \widetilde{\Pi}_{p-1}(\mathbb{C})$,

$$\widetilde{L}_k^{AB}(z) := \prod_{\substack{j=0 \\ j \neq k}}^{p-1} \frac{z - z_j^{AB}}{z_k^{AB} - z_j^{AB}}, \tag{2.16}$$

$$\mathcal{I}_p^{AB} \widetilde{g} := \sum_{j=0}^{p-1} \widetilde{g}(z_j^{AB}) \widetilde{L}_j^{AB}. \tag{2.17}$$

We have the following result.

LEMMA 2.3. *Let $p \in \mathbb{N}$, $p \geq 3$, two boxes $A, B \subset \mathbb{R}$ be admissible in the sense $w^A w^B \leq N$, and the Lagrange functions $l_r^{AB} : A \to \mathbb{C}$,*

$$l_r^{AB}(x) := \widetilde{L}_r^{AB}(z(x)), \quad r = 0, \ldots, p-1, \tag{2.18}$$

be given. Then, the interpolation operator (2.13) *has the representation*

$$\mathcal{J}_p^{AB} g(x) = \mathrm{e}^{2\pi \mathrm{i} \left(c^B + \frac{w^B}{2}\right) x/N} \sum_{r=0}^{p-1} g(x_r^A) \mathrm{e}^{-2\pi \mathrm{i} \left(c^B + \frac{w^B}{2}\right) x_r^A/N} l_r^{AB}(x) \tag{2.19}$$

and its operator norm is bounded by

$$\|\mathcal{J}_p^{AB}\| := \sup_{g \in C(A) \setminus \{0\}} \frac{\|\mathcal{J}_p^{AB} g\|_{C(A)}}{\|g\|_{C(A)}} \leq C_p, \quad C_p := \sqrt{K_p} \left(1 + \frac{2}{\pi} \log p\right), \tag{2.20}$$

where

$$K_p := \left(\frac{2\pi^2}{\left(1 - \cos \frac{2\pi}{p-1}\right)(p-1)^2} \right)^{p-1}, \quad K_p \leq \frac{\pi^4}{16}, \quad \lim_{p \to \infty} K_p = 1. \tag{2.21}$$

Proof. Let $v : \mathbb{C} \to \mathbb{C}$ be continuous with $v(z) = v(z(x)) = g(x)$ for $x \in A$. The polynomial $q \in \widetilde{\Pi}_{p-1}(\mathbb{C})$, which interpolates the points $(z_r^{AB}, v(z_r^{AB})) \in \mathbb{C} \times \mathbb{C}$, $r = 0, \ldots, p-1$, is unique and given by

$$q(z) = \sum_{r=0}^{p-1} v(z_r^{AB}) \widetilde{L}_r(z) = \sum_{r=0}^{p-1} g(x_r^A) l_r^{AB}(x).$$

The assertion follows, since the function

$$\mathrm{e}^{2\pi\mathrm{i}\left(c^B+\frac{w^B}{2}\right)\frac{x}{N}}\cdot q(z(x))\cdot \mathrm{e}^{-2\pi\mathrm{i}\left(c^B+\frac{w^B}{2}\right)\frac{x_r^A}{N}}$$

lies in $\Pi_B^p(A)$ and interpolates the function g in the nodes x_r^A, $r=0,\dots,p-1$. Furthermore, we have

$$\begin{aligned}\max_{x\in A}|\mathcal{J}_p^{AB}g(x)| &= \max_{x\in A}\left|\mathrm{e}^{2\pi\mathrm{i}\left(c^B+\frac{w^B}{2}\right)x/N}\sum_{r=0}^{p-1}g(x_r^A)\mathrm{e}^{-2\pi\mathrm{i}\left(c^B+\frac{w^B}{2}\right)x_r^A/N}l_r^{AB}(x)\right| \\ &\le \|g\|_{C(A)}\max_{x\in A}\sum_{r=0}^{p-1}|l_r^{AB}(x)|.\end{aligned}$$

Without loss of generality, let now the box B be such that $w^Aw^B=N$. Using $x_r^A=c^A+\alpha_r w^A$, the mapping $y:A\to[-\frac{1}{2},\frac{1}{2}]$, and the normalised Lagrange functions $l_r:[-\frac{1}{2},\frac{1}{2}]\to\mathbb{C}$,

$$y(x) := \frac{1}{w^A}(x-c^A)=\frac{w^B}{N}(x-c^A), \tag{2.22}$$

$$l_r(y) := l_r^{AB}(x(y)) = \prod_{\substack{j=0\\ j\neq r}}^{p-1}\frac{\mathrm{e}^{-2\pi\mathrm{i}\frac{y}{p-1}}-\mathrm{e}^{-2\pi\mathrm{i}\frac{\alpha_j}{p-1}}}{\mathrm{e}^{-2\pi\mathrm{i}\frac{\alpha_r}{p-1}}-\mathrm{e}^{-2\pi\mathrm{i}\frac{\alpha_j}{p-1}}}, \tag{2.23}$$

yields the relation

$$|l_r^{AB}(x)|^2=|l_r(y)|^2=\prod_{\substack{j=0\\ j\neq r}}^{p-1}\frac{1-\cos\left(\frac{2\pi}{p-1}(y-\alpha_j)\right)}{1-\cos\left(\frac{2\pi}{p-1}(\alpha_r-\alpha_j)\right)}.$$

Since $y-\alpha_j\in[-1,1]$ and $\alpha_r-\alpha_j\in[-1,1]$, we apply Lemma 2.1, estimates (2.5) and (2.4), to obtain

$$\begin{aligned}&\le \prod_{\substack{j=0\\ j\neq r}}^{p-1}\frac{4\pi^2}{2\left(1-\cos\frac{2\pi}{p-1}\right)(p-1)^2}\frac{(y-\alpha_j)^2}{(\alpha_j-\alpha_s)^2} \\ &= K_p\prod_{\substack{j=0\\ j\neq r}}^{p-1}\left(\frac{2y-t_j}{t_r-t_j}\right)=K_p(L_r(2y))^2.\end{aligned}$$

The assertion follows by Lemma 2.2 estimate (2.9) in

$$\max_{x\in A}\sum_{r=0}^{p-1}|l_r^{AB}(x)|\le\sqrt{K_p}\max_{x\in[-1,1]}\sum_{r=0}^{p-1}|L_r(x)|\le\sqrt{K_p}(1+\frac{2}{\pi}\log p).$$

Setting $x=\frac{2\pi}{p-1}$ in Lemma 2.1 (2.6) finally yields $\lim_{p\to\infty}K_p=1$ and $K_p\le\frac{\pi^4}{16}$. □

REMARK 2.4. *In [17], the extremal points $t_j^{\max}=\cos\frac{j}{p}\pi$, $j=0,\dots,p$, of the Chebyshev polynomial were used in space and frequency domain. This yields a globally continuous approximant. In contrast, we use the Chebyshev nodes in space and*

equispaced nodes in frequency domain. This gives a close connection to polynomial interpolation in the complex plane and thus allows for the subsequent error analysis. Moreover, the modification to equispaced nodes in frequency domain allows for an explicit, stable, and effective representation of the trigonometric interpolation operator in a Lagrange type basis.

In contrast to [2, Thm. 3], where an interpolation by means of Lagrange polynomials with real nodes is used, we always interpolate with respect to the real spatial variable x and by means of our Lagrange functions l_r^{AB}, which are Lagrange polynomials with complex nodes via the mapping (2.15)*. In particular, interpolating a function from $\Pi_B(A)$ yields a function in its subspace $\Pi_B^p(A)$.*

For spatial dimensions $d > 1$, a box is given as a Cartesian product $A = A^{(1)} \times \ldots \times A^{(d)}$, where $A^{(k)} = [a_k, b_k]$, $k = 0, \ldots, d$, are one-dimensional boxes. We define the center and the width by

$$\boldsymbol{c}^A := \frac{1}{2}(a_1 + b_1, \ldots, a_d + b_d)^\top, \quad w^A := \operatorname{diam}_\infty A := \max_{k=1,\ldots,d}(b_k - a_k),$$

respectively. For boxes $A, B \subset \mathbb{R}^d$, we use tensor products of the spaces $\Pi_B(A)$ and $\Pi_B^p(A)$ and define the interpolation operator in a straightforward manner by

$$\mathcal{J}_p^{AB} = \bigotimes_{r=1}^{d} \mathcal{J}_p^{A^{(r)}B^{(r)}}.$$

2.2. Error analysis. In [17] a Taylor expansion of the complex exponential function in the real variable has been used to motivate a restriction on the product of the widths of the boxes A and B. Subsequently, we present an error estimate for the interpolation $\mathcal{J}_p^{AB} g$ if $g \in \Pi_B(A)$ and A, B fulfil such an admissibility condition. Its main ingredient is the following Taylor expansion of the power function on the unit circle.

LEMMA 2.5. *Let $p \in \mathbb{N}$, $p \geq 5$, $\Gamma_p := \{z \in \mathbb{C} : z = \mathrm{e}^{-2\pi \mathrm{i} x/(p-1)}, -\frac{1}{2} \leq x \leq \frac{1}{2}\}$, and $\alpha \in [0, p-1]$, then we have for $z \in \Gamma_p$ the estimate*

$$\left| z^\alpha - \sum_{k=0}^{p-1} \binom{\alpha}{k} (z-1)^k \right| \leq c_p$$

with the constant

$$c_p := \frac{1}{\pi p} \left(\frac{\pi}{p-1} \right)^p. \tag{2.24}$$

Proof. The function $g : \mathbb{C} \setminus (-\infty, 0] \to \mathbb{C}$, $g(z) := z^\alpha$, is holomorphic and can be represented by its Taylor series at $z = 1$ in Γ_p for $p \geq 5$. Using the estimate (2.4), yields

$$|z-1|^2 = 2\left(1 - \cos\frac{2\pi x}{p-1}\right) \leq \left(\frac{2\pi x}{p-1}\right)^2 \leq \left(\frac{\pi}{p-1}\right)^2 < 1$$

and we finally follow the proof of [15, Thm. 1] to obtain

$$\left| z^\alpha - \sum_{k=0}^{p-1} \binom{\alpha}{k} (z-1)^k \right| \leq \sum_{k=p}^{\infty} \left| \binom{\alpha}{k} + \binom{\alpha}{k+1} \right| \frac{\left|(1-z)^p - (1-z)^{k+1}\right|}{|z|}$$

$$\leq 2|z-1|^p \left| \binom{\alpha}{p} \right| \leq \frac{2|z-1|^p}{2\pi p},$$

where the last estimate can be proven by induction over $p \geq 5$. ☐

THEOREM 2.6. *Let $p, N \in \mathbb{N}$, $p \geq 5$, two boxes $A, B \subset \mathbb{R}^d$ be admissible in the sense*

$$w^A w^B \leq N,$$

and $g \in \Pi_B(A)$, $g(\boldsymbol{x}) := \sum_{k=1}^{M_2} \hat{g}_k \mathrm{e}^{2\pi \mathrm{i} \boldsymbol{\xi}_k \boldsymbol{x}/N}$, $\hat{g}_k \in \mathbb{C}$, $k = 1, \ldots, M_2$, then we have the error estimate

$$\|g - \mathcal{J}_p^{AB} g\|_{C(A)} \leq \frac{(1+C_p)(C_p^d - 1)}{C_p - 1} \cdot c_p \cdot \|\hat{\boldsymbol{g}}\|_1,$$

where the constants are given by (2.20) *and* (2.24)*, respectively.*

Proof. Without loss of generality, let the box B be such that $w^A w^B = N$. We start with the univariate case $d = 1$ and shift and dilate $A \mapsto [-\frac{1}{2}, \frac{1}{2}]$ and $B \mapsto [-\frac{N}{2}, \frac{N}{2}]$. Together with $\widetilde{g} : [-\frac{1}{2}, \frac{1}{2}] \to \mathbb{C}$, $\widetilde{g}(y) := \sum_{k=1}^{M_2} \hat{g}_k \mathrm{e}^{2\pi \mathrm{i} \xi_k c^A/N} \mathrm{e}^{2\pi \mathrm{i} \xi_k y / w^B}$, this yields

$$\mathcal{J}_p^{AB} g(x) = \mathrm{e}^{2\pi \mathrm{i} c^B x/N} \mathcal{J}_p \widetilde{g}(y), \quad y := \frac{1}{w^A}(x - c^A),\ \mathcal{J}_p := \mathcal{J}_p^{[-\frac{1}{2},\frac{1}{2}][-\frac{N}{2},\frac{N}{2}]}.$$

Now, we map $[-\frac{1}{2}, \frac{1}{2}] \mapsto \Gamma_p$ and set $h : \Gamma_p \to \mathbb{C}$, $h(z) := z^{\frac{p-1}{2}} \sum_{k=1}^{M_2} \hat{h}_k z^{-(p-1)\xi_k/w^B}$, $\hat{h}_k := \hat{g}_k \mathrm{e}^{2\pi \mathrm{i} \xi_k c^A/N}$, which leads to

$$\mathcal{J}_p \widetilde{g}(y) = z^{-\frac{p-1}{2}} \mathcal{I}_p h(z), \quad z := \mathrm{e}^{-2\pi \mathrm{i} y/(p-1)},\ \mathcal{I}_p := \mathcal{I}_p^{[-\frac{1}{2},\frac{1}{2}][-\frac{N}{2},\frac{N}{2}]}.$$

Both mappings leave the error unchanged, i.e.,

$$\max_{x \in A} |g(x) - \mathcal{J}_p^{AB} g(x)| = \max_{y \in [-\frac{1}{2},\frac{1}{2}]} |\widetilde{g}(y) - \mathcal{J}_p \widetilde{g}(y)| = \max_{z \in \Gamma_p} |h(z) - \mathcal{I}_p h(z)|.$$

We rewrite $h(z) = \sum_{k=1}^{M_2} \hat{h}_k z^{\eta_k}$ with $\eta_k \in [0, p-1]$, and approximate h by its truncated Taylor series $h_p \in \widetilde{\Pi}_{p-1}(\mathbb{C})$ at $z = 1$,

$$h_p(z) := \sum_{k=1}^{M_2} \hat{h}_k \sum_{r=0}^{p-1} \binom{\eta_k}{r} (z-1)^r.$$

Due to the reproduction of polynomials $\mathcal{I}_p h_p = h_p$ and the bound on the operator norm, cf. proof of Lemma 2.3,

$$\|\mathcal{I}_p\| := \sup_{\substack{h \in C(\Gamma_p) \\ \|h\|_{C(\Gamma_p)} = 1}} \|\mathcal{I}_p h\|_{C(\Gamma_p)} = \|\mathcal{J}_p^{AB}\| \leq C_p,$$

Lemma 2.5 yields the assertion by

$$\begin{aligned} \max_{z \in \Gamma_p} |h(z) - \mathcal{I}_p h(z)| &\leq \max_{z \in \Gamma_p} |h(z) - h_p(z)| + \max_{z \in \Gamma_p} |h_p(z) - \mathcal{I}_p h(z)| \\ &\leq (1 + \|\mathcal{I}_p\|) \max_{z \in \Gamma_p} |h(z) - h_p(z)| \\ &\leq (1 + C_p) c_p \sum_{k=1}^{M_2} |\hat{g}_k|. \end{aligned}$$

Now, let $d > 1$ and $B = B^{(1)} \times \ldots \times B^{(d)}, A = A^{(1)} \times \ldots \times A^{(d)} \subset [0, N]^d$ be admissible. Since $\mathcal{J}_p^{AB} = \mathcal{J}_p^{A^{(1)}B^{(1)}} \otimes \ldots \otimes \mathcal{J}_p^{A^{(d)}B^{(d)}}$, we immediately have $\|\mathcal{J}_p^{AB}\| \leq C_p^d$. By slight abuse of notation we write $\mathcal{J}_p^{A^{(\nu)}B^{(\nu)}}$ also for the interpolation of a d-variate function in its ν-th variable and obtain by

$$\begin{aligned}
\left\|g - \mathcal{J}_p^{AB} g\right\|_{C(A)} &\leq \left\|g - \mathcal{J}_p^{A^{(1)}B^{(1)}} g\right\|_{C(A)} + \left\|\mathcal{J}_p^{A^{(1)}B^{(1)}} g - \mathcal{J}_p^{AB} g\right\|_{C(A)} \\
&\leq \sum_{\nu=1}^{d} \prod_{\mu=1}^{\nu-1} \left\|\mathcal{J}_p^{A^{(\mu)}B^{(\mu)}}\right\| \left\|g - \mathcal{J}_p^{A^{(\nu)}B^{(\nu)}} g\right\|_{C(A)} \\
&\leq (1 + C_p) c_p \|\hat{\boldsymbol{g}}\|_1 \sum_{\nu=1}^{d} C_p^{\nu-1}
\end{aligned}$$

the final error estimate. □

2.3. Realisation. The local approximation by means of the interpolation operator needs to be realised using a basis for the ansatz space $\Pi_B^p(A)$. Subsequently, we discuss a variant of the original approach [17] which uses a monomial type basis and a new variant which relies on a Lagrange type basis. While both approaches take approximately the same amount of computation, the latter is much more stable. In both cases, the univariate realisation generalises easily to the multivariate case since the tensor product structure of the interpolation operator just turns into a Kronecker product structure of the involved matrices.

Section 3 considers the butterfly scheme built upon the dyadic decomposition of the spatial domain X and the frequency domain T. For $A \subset X$ and $B \subset T$ admissible, this asks for the approximation $u^{AB} \in \Pi_B(A)$,

$$u^{AB} := \mathcal{J}_p^{AB} \sum_{S \in S_B} u^{PS}, \tag{2.25}$$

where

$$S_B := \left\{ \left[c^B - \frac{w^B}{2}, c^B \right], \left[c^B, c^B + \frac{w^B}{2} \right] \right\},$$

denotes the set of sons, for $d = 1$ at most two, of the set of frequencies

$$B = \left[c^B - \frac{w^B}{2}, c^B + \frac{w^B}{2} \right]$$

and the interpolation error is small in each of the spatial sets, for $d = 1$ again at most two,

$$A = \left[c^A - \frac{w^A}{2}, c^A + \frac{w^A}{2} \right],$$

which are subsets of their father

$$P := \left[c^P - \frac{w^P}{2}, c^P + \frac{w^P}{2} \right].$$

Subsequently, we rely on the admissibility condition $w^A w^B = N$ and on the dyadic decomposition which results in $w^P w^B = 2N$, see Figure 2.1 for an illustration of the sets.

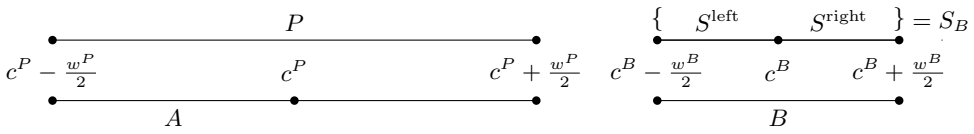

FIGURE 2.1. *Illustration of the spatial set $A \subset P$ and frequency set $B \supset S_B$.*

2.3.1. Monomial type basis. We closely follow the discussion in [17, Sect. 3.2] for solving the interpolation problem. The interpolant $\mathcal{J}_p^{AB} g$ for a function $g \in \Pi_B(A)$ is given by $g^{AB}(x) = \sum_{s=0}^{p-1} \hat{g}_s^{AB} \mathrm{e}^{2\pi \mathrm{i} \xi_s^B x/N}(x)$ with the coefficient vector

$$\begin{aligned} \hat{\boldsymbol{g}}^{AB} &= \big(f_s^{AB}\big)_{s=0}^{p-1} = (\boldsymbol{M}^{AB})^{-1} \boldsymbol{g}^{AB}, \quad \boldsymbol{g}^{AB} = \big(g(x_r^A)\big)_{r=0}^{p-1}, \\ \boldsymbol{M}^{AB} &:= \Big(\mathrm{e}^{2\pi \mathrm{i} \xi_s^B x_r^A/N}\Big)_{r,s=0}^{p-1}, \end{aligned} \tag{2.26}$$

where we use the equally spaced nodes $\xi_s^B \in B$ and Chebyshev nodes $x_r^A \in A$, cf. (2.12) and (2.14). Using the two diagonal matrices

$$\boldsymbol{D}_1^{AB} := \operatorname{diag}\Big(\mathrm{e}^{2\pi \mathrm{i}(c^A + \alpha_r w^A) c^B/N}\Big)_{r=0}^{p-1}, \quad \boldsymbol{D}_2^{AB} := \operatorname{diag}\Big(\mathrm{e}^{2\pi \mathrm{i} c^A \beta_s w^B/N}\Big)_{s=0}^{p-1},$$

the matrix $\boldsymbol{M}^{AB} \in \mathbb{C}^{p\times p}$ can be factorised as

$$\boldsymbol{M}^{AB} = \boldsymbol{D}_1^{AB} \boldsymbol{G} \boldsymbol{D}_2^{AB}, \quad \boldsymbol{G} := \big(\mathrm{e}^{2\pi \mathrm{i} \alpha_r \beta_s}\big)_{r,s=0}^{p-1}, \tag{2.27}$$

where the matrix $\boldsymbol{G} \in \mathbb{C}^{p\times p}$ is independent of A and B. Applied to (2.25), this yields

$$\hat{\boldsymbol{u}}^{AB} = \Big(\boldsymbol{D}_2^{AB}\Big)^{-1} \boldsymbol{G}^{-1} \Big(\boldsymbol{D}_1^{AB}\Big)^{-1} \boldsymbol{u}^{AB}, \quad \boldsymbol{u}^{AB} = \left(\sum_{S\in S_B} u^{PS}(x_r^A)\right)_{r=0}^{p-1}.$$

Given the coefficients $\hat{\boldsymbol{u}}^{PS} = (\hat{u}_s^{PS})_{s=0}^{p-1} \in \mathbb{C}^p$ in $u^{PS}(x) = \sum_{s=0}^{p-1} \hat{u}_s^{PS} \mathrm{e}^{2\pi \mathrm{i} \xi_s^S x/N}$, we compute

$$\boldsymbol{u}^{AB} = \sum_{S\in S_B} \boldsymbol{N}^{AS} \hat{\boldsymbol{u}}^{PS}, \quad \boldsymbol{N}^{AS} := \Big(\mathrm{e}^{2\pi \mathrm{i} \xi_s^S x_r^A/N}\Big)_{r,s=0}^{p-1}.$$

Again, using two diagonal matrices

$$\boldsymbol{E}_1^{AS} := \operatorname{diag}\Big(\mathrm{e}^{2\pi \mathrm{i}(c^A + \alpha_r w^A) c^S/N}\Big)_{r=0}^{p-1}, \quad \boldsymbol{E}_2^{AS} := \operatorname{diag}\Big(\mathrm{e}^{2\pi \mathrm{i} c^A \beta_s w^S/N}\Big)_{s=0}^{p-1},$$

we have a factorisation

$$\boldsymbol{N}^{AS} = \boldsymbol{E}_1^{AS} \boldsymbol{H} \boldsymbol{E}_2^{AS}, \quad \boldsymbol{H} := \big(\mathrm{e}^{\pi \mathrm{i} \alpha_r \beta_s}\big)_{r,s=0}^{p-1},$$

where the matrix $\boldsymbol{H} \in \mathbb{C}^{p\times p}$ is independent of A and B. Altogether, this yields

$$\hat{\boldsymbol{u}}^{AB} = (\boldsymbol{D}_2^{AB})^{-1} \boldsymbol{G}^{-1} \sum_{S\in S_B} \boldsymbol{C}^{AS} \boldsymbol{H} \boldsymbol{E}_2^{AS} \hat{\boldsymbol{u}}^{PS}, \quad \boldsymbol{C}^{AS} = \operatorname{diag}\left(\mathrm{e}^{\mp \pi \mathrm{i}\left(\frac{c^A}{w^A} + \alpha_r\right)/2}\right)_{r=0}^{p-1}, \tag{2.28}$$

where we have used

$$c^S - c^B = \begin{cases} -\frac{w^S}{2} & S \text{ is the left son of } B, \\ \frac{w^S}{2} & S \text{ is the right son of } B. \end{cases}$$

2.3.2. Lagrange type basis. Our new approach relies more directly on the definition (2.19) of the interpolant $\mathcal{J}_p^{AB} g$ for a function $g \in \Pi_B(A)$. Applied to (2.25) and in contrast to the variant above, the functions $u^{PS} \in \Pi_S(P)$, $S \in S_B$, are given by their function values $u^{PS}(x_r^P)$, $r = 0, \dots, p-1$, at the Chebyshev nodes in P and we compute the function values $u^{AB}(x_r^A)$, $r = 0, \dots, p-1$, at Chebyshev nodes in A. More detailed, we have

$$u^{AB}(x_r^A) = \sum_{S \in S_B} \mathrm{e}^{2\pi \mathrm{i}\left(c^S + \frac{w^S}{2}\right) x_r^A / N} \sum_{s=0}^{p-1} u^{PS}(x_s^P) \mathrm{e}^{-2\pi \mathrm{i}\left(c^S + \frac{w^S}{2}\right) x_s^P / N} \cdot l_s^{PS}(x_r^A). \quad (2.29)$$

The Lagrange polynomials are given via the mapping (2.15) by

$$l_s^{PS}(x_r^A) = \prod_{\substack{j=0 \\ j \neq s}}^{p-1} \frac{z(x_r^A) - z(x_j^P)}{z(x_s^P) - z(x_j^P)}.$$

Inserting $x_r^A = c^A + \alpha_r w^A$ and $x_j^P = c^P + \alpha_j w^P$ and using

$$c^A - c^P = \begin{cases} -\frac{w^A}{2} & A \text{ is the left son of } P, \\ \frac{w^A}{2} & A \text{ is the right son of } P, \end{cases}$$

yields

$$l_s^{PS}(x_r^A) = \begin{cases} \prod\limits_{\substack{j=0 \\ j \neq s}}^{p-1} \frac{\mathrm{e}^{-\pi \mathrm{i}\left(\alpha_r - \frac{1}{2}\right)/(p-1)} - \mathrm{e}^{-2\pi \mathrm{i} \frac{\alpha_j}{p-1}}}{\mathrm{e}^{-2\pi \mathrm{i} \frac{\alpha_s}{p-1}} - \mathrm{e}^{-2\pi \mathrm{i} \frac{\alpha_j}{p-1}}} & A \text{ is the left son of } P, \\ \prod\limits_{\substack{j=0 \\ j \neq s}}^{p-1} \frac{\mathrm{e}^{-\pi \mathrm{i}\left(\alpha_r + \frac{1}{2}\right)/(p-1)} - \mathrm{e}^{-2\pi \mathrm{i} \frac{\alpha_j}{p-1}}}{\mathrm{e}^{-2\pi \mathrm{i} \frac{\alpha_s}{p-1}} - \mathrm{e}^{-2\pi \mathrm{i} \frac{\alpha_j}{p-1}}} & A \text{ is the right son of } P. \end{cases} \quad (2.30)$$

With the vectors

$$\boldsymbol{u}^{PS} = \left(u^{PS}(x_r^P)\right)_{r=0}^{p-1}, \quad \boldsymbol{u}^{AB} = \left(u^{AB}(x_r^A)\right)_{r=0}^{p-1},$$

the diagonal matrices

$$\boldsymbol{R}^{AS} := \operatorname{diag}\left(\mathrm{e}^{2\pi \mathrm{i}\left(c^S + \frac{w^S}{2}\right) x_r^A / N}\right)_{r=0}^{p-1}, \quad \boldsymbol{S}^{PS} := \operatorname{diag}\left(\mathrm{e}^{-2\pi \mathrm{i}\left(c^S + \frac{w^S}{2}\right) x_s^P / N}\right)_{s=0}^{p-1},$$

and the Lagrange matrix, which depends only on the relation between A and P,

$$\boldsymbol{L}^A := \left(l_s^{PS}(x_r^A)\right)_{r,s=0}^{p-1}, \quad (2.31)$$

we finally obtain

$$\boldsymbol{u}^{AB} = \sum_{S \in S_B} \boldsymbol{R}^{AS} \boldsymbol{L}^A \boldsymbol{S}^{PS} \boldsymbol{u}^{PS}. \quad (2.32)$$

2.3.3. Computational complexity. The computation of the coefficients $\hat{\boldsymbol{u}}^{AB}$ from the coefficients $\hat{\boldsymbol{u}}^{PS}$ in (2.28) takes $\mathcal{O}(p^2)$ arithmetic operations, once the two matrices $\boldsymbol{G}^{-1}, \boldsymbol{H} \in \mathbb{C}^{p\times p}$ are set up. Similarly, the evaluation of $\boldsymbol{u}^{AB}$ from the function values $\boldsymbol{u}^{PS}$ in (2.32) takes $\mathcal{O}(p^2)$ arithmetic operations after precomputing the two Lagrange matrices $\boldsymbol{L}^A \in \mathbb{C}^{p\times p}$, $A \subset P$. Using the tensor product structure of the interpolation operator, the multivariate case clearly takes $\mathcal{O}(p^{d+1})$ arithmetic operations, see also [11] for an introduction to tensor and n-mode products.

Moreover, the matrices $\boldsymbol{G}^{-1}, \boldsymbol{H}, \boldsymbol{L}^A \in \mathbb{C}^{p\times p}$ are of Cauchy-Vandermonde type and thus allow for matrix vector multiplications in only $Cp\log^2 p$ floating point operations, cf. [7]. However note that p is hardly large enough in order that this consideration pays off in practice.

2.4. Stability. While implementing the original scheme [17], we found that the final accuracy of the butterfly sparse FFT is limited far above machine accuracy as shown in Section 4. Of course, the error of the local approximation and thus of the butterfly scheme decreases rapidly with increasing local expansion degree p - at least in precise arithmetic. On the other hand, we show subsequently that the condition number of the interpolation matrix $\boldsymbol{M}^{AB}$ strongly increases and thus rounding errors take over for larger p. Alternatively, we prove a weaker increase of the condition number of the Lagrange matrix $\boldsymbol{L}^A$ which seems to suffice for a stable butterfly sparse FFT. Based on the Lemmata 2.1, 2.2, we are prepared to prove the following bound on the stability of the local approximation scheme when the monomial type basis is used.

THEOREM 2.7. *Let $p \in \mathbb{N}$, $p \geq 3$, and the local boxes be given as in Section 2.3. The spectral condition number of the interpolation matrix $\boldsymbol{M}^{AB} \in \mathbb{C}^{p\times p}$ given in* (2.26) *fulfils*

$$\kappa(\boldsymbol{M}^{AB}) \geq \begin{cases} \sqrt{p}\left(\dfrac{p-1}{2\pi}\right)^{p-1} & p \geq 3, \qquad (2.33) \\ \dfrac{1}{\sqrt{p}}\left(\dfrac{2(p-1)}{\pi}\right)^{p-1} & p \geq 3 \text{ and odd.} \qquad (2.34) \end{cases}$$

Proof. We use the factorisations $\boldsymbol{M}^{AB} = \boldsymbol{D}_1^{AB}\boldsymbol{G}\boldsymbol{D}_2^{AB}$, see (2.27), and

$$\boldsymbol{G} = \boldsymbol{D}\boldsymbol{V}, \quad \boldsymbol{D} = \operatorname{diag}((\mathrm{e}^{\pi \mathrm{i}\alpha_r})_{r=0}^{p-1}), \quad \boldsymbol{V} = (z_r^s)_{r,s=0}^{p-1}, \quad z_r := \mathrm{e}^{-2\pi\mathrm{i}\frac{\alpha_r}{p-1}}.$$

Noting, that the norm of all the diagonal matrices and their inverses is equal to one, it suffices to analyse the Vandermonde matrix $\boldsymbol{V}$. We have

$$\|\boldsymbol{V}\|_2 = \sup_{\boldsymbol{x}\in\mathbb{C}^p\setminus\{0\}} \frac{\|\boldsymbol{V}\boldsymbol{x}\|_2}{\|\boldsymbol{x}\|_2} \geq \frac{\|\boldsymbol{V}\boldsymbol{e}_0\|_2}{\|\boldsymbol{e}_0\|_2} = \sqrt{p}.$$

for the zeroth unit vector $\boldsymbol{e}_0 = (1, 0, \ldots, 0)^\top \in \mathbb{C}^p$ and bound the norm $\|\boldsymbol{V}^{-1}\|_2$ by a similar technique.

Solving the linear system $\boldsymbol{V}\boldsymbol{f} = \boldsymbol{e}_0$ is equivalent to the polynomial interpolation problem

$$q : \mathbb{C} \to \mathbb{C}, \quad q(z) = \sum_{s=0}^{p-1} f_s z^s, \quad \text{such that} \quad q(z_r) = \delta_{r,0} \text{ for } r = 0, \ldots, p-1. \qquad (2.35)$$

In terms of the Lagrange polynomials to the nodes $\{z_r\}_{r=0}^{p-1}$, its solution is given by

$$q(z) = \widetilde{L}_0(z) = \prod_{r=1}^{p-1} \frac{z - z_r}{z_0 - z_r} = \left(\prod_{r=1}^{p-1} \frac{1}{z_0 - z_r} \right) z^{p-1} + \dots \quad .$$

and we consider the leading coefficient $f_{p-1} = \prod_{r=1}^{p-1} \frac{1}{z_0 - z_r}$ in the monomial expansion (2.35). Applying Lemma 2.1, estimates (2.3) and (2.4), yields

$$\begin{aligned} |z_0 - z_r|^2 &= 2 - 2\cos\left(\frac{\pi}{p-1} \left(\cos\frac{\pi}{2p} - \cos\frac{2r+1}{2p}\pi \right) \right) \\ &\leq 2 - 2\cos\frac{2\pi}{p-1} \leq 2 - 2\left(1 - \frac{4\pi^2}{2(p-1)^2} \right) = \left(\frac{2\pi}{p-1} \right)^2 . \end{aligned}$$

Hence, we obtain

$$\|\boldsymbol{V}^{-1}\|_2 \geq \|\boldsymbol{V}^{-1}\boldsymbol{e}_0\|_2 \geq |f_{p-1}| = \prod_{r=1}^{p-1} \frac{1}{|z_0 - z_r|} \geq \left(\frac{p-1}{2\pi} \right)^{p-1}$$

and thus the assertion (2.33).

For $p = 2n+1$, $n \in \mathbb{N}$, we consider the linear system $\boldsymbol{V}\boldsymbol{f} = \boldsymbol{e}_n$ with the n-th unit vector, which is equivalent to the interpolation problem

$$q : \mathbb{C} \to \mathbb{C}, \quad q(z) = \sum_{s=0}^{p-1} f_s z^s, \quad \text{such that} \quad q(z_r) = \delta_{n,r} \text{ for } r = 0, \dots, p-1.$$

Noting $z_n = 1$ and analogously to the above consideration, we have

$$q(z) = \widetilde{L}_n(z) = \prod_{\substack{k=0 \\ k \neq n}}^{p-1} \frac{z - z_k}{1 - z_k} = f_{p-1} z^{p-1} + \dots \quad , \; f_{p-1} = \prod_{\substack{k=0 \\ k \neq n}}^{p-1} \frac{1}{1 - z_k}.$$

Using Lemma 2.1 (2.4) yields

$$|1 - z_k|^2 = 2 - 2\cos\frac{\pi}{p-1} t_k \leq \frac{\pi^2}{(p-1)^2} t_k^2$$

and together with Lemma 2.2 (2.7) in

$$\|\boldsymbol{V}^{-1}\|_2 \geq |f_{p-1}| \geq \left(\frac{p-1}{\pi} \right)^{p-1} \prod_{\substack{k=0 \\ k \neq n}}^{p-1} |t_k|^{-1} = \frac{2^{p-1}}{p} \left(\frac{p-1}{\pi} \right)^{p-1}$$

the assertion (2.34) follows. □

The condition number of the matrix $\boldsymbol{N}^{AS}$ in Section 2.3.1 can be analysed in the same way to yield $\kappa(\boldsymbol{N}^{AS}) \approx 2^{p-1}\kappa(\boldsymbol{M}^{AB})$. In contrast to the lower bound on the conditioning of the original method, we obtain an upper bound for the local approximation scheme when the Lagrange type basis, cf. Section 2.3.2, is used.

THEOREM 2.8. *Under the assumptions of Theorem 2.7, the spectral condition number of the Lagrange interpolation matrix* $\boldsymbol{L}^A \in \mathbb{C}^{p \times p}$ *given in* (2.31) *fulfils*

$$\kappa(\boldsymbol{L}^A) \leq K_p \frac{\sqrt{2p \cdot 34^p}}{4} \leq \frac{\sqrt{2p}}{4} \cdot 6^{p+1}.$$

Proof. The Lagrange functions (2.30) are independent of the box A, up to its relation to the father box P. Setting $x_r = \alpha_r \mp \frac{1}{2}$ in (2.30) yields

$$|l_s^{PS}(x_r^A)|^2 = \prod_{\substack{j=0\\ j\neq s}}^{p-1} \frac{1-\cos\left(\frac{2\pi}{p-1}(\alpha_j - \frac{x_r}{2})\right)}{1-\cos\left(\frac{2\pi}{p-1}(\alpha_j - \alpha_s)\right)}.$$

Since $x_r \in [-1,1]$ and thus $\alpha_j - \frac{x_r}{2} \in [-1,1]$, we can follow the ideas in the proof of Lemma 2.3 to obtain the relation

$$\leq K_p \prod_{\substack{j=0\\ j\neq s}}^{p-1} \left(\frac{x_r - t_j}{t_s - t_j}\right)^2 = K_p \cdot (L_s(x_r))^2 .$$

Due to inequality (2.8) in Lemma 2.2, this yields

$$\|\boldsymbol{L}^A\|_{\mathrm{F}}^2 = \sum_{r=0}^{p-1}\sum_{s=0}^{p-1} |l_s^{PS}(x_r^A)|^2 \leq K_p \sum_{r=0}^{p-1} \max_{x\in[-1,1]} \sum_{s=0}^{p-1} (L_s(x))^2 \leq 2pK_p. \tag{2.36}$$

In view of the related polynomial interpolation problem on the complex unit circle and by changing the basis of the Lagrange polynomials l_s^{PS} to l_s^{AS}, the entries of the inverse Lagrange matrix can be written as

$$\left(\left(\boldsymbol{L}^A\right)^{-1}\right)_{r,s} = l_s^{AS}(x_r^P) = \begin{cases} \prod\limits_{\substack{j=0\\ j\neq s}}^{p-1} \frac{\mathrm{e}^{-\pi\mathrm{i}\left(2\alpha_r+\frac{1}{2}\right)/(p-1)} - \mathrm{e}^{-\pi\mathrm{i}\frac{\alpha_j}{p-1}}}{\mathrm{e}^{-\pi\mathrm{i}\frac{\alpha_s}{p-1}} - \mathrm{e}^{-\pi\mathrm{i}\frac{\alpha_j}{p-1}}} & A \text{ is the left son of } P, \\ \prod\limits_{\substack{j=0\\ j\neq s}}^{p-1} \frac{\mathrm{e}^{-\pi\mathrm{i}\left(2\alpha_r-\frac{1}{2}\right)/(p-1)} - \mathrm{e}^{-\pi\mathrm{i}\frac{\alpha_j}{p-1}}}{\mathrm{e}^{-\pi\mathrm{i}\frac{\alpha_s}{p-1}} - \mathrm{e}^{-\pi\mathrm{i}\frac{\alpha_j}{p-1}}} & A \text{ is the right son of } P. \end{cases}$$

Analogously to the first part of the proof, we set $x_r = 2\alpha_r \pm \frac{1}{2} \subset \left[-\frac{3}{2}, \frac{3}{2}\right]$ and use $1/2(\alpha_j - x_r) \in [-1,1]$ to use again the ideas in proof of Lemma 2.3. Together with $2x_r \in [-3,3]$, inequality (2.10) in Lemma 2.2 yields

$$|l_s^{AS}(x_r^P)|^2 = \prod_{\substack{j=0\\ j\neq s}}^{p-1} \frac{1-\cos\left(\frac{2\pi}{p-1}(\frac{\alpha_j}{2} - \frac{x_r}{2})\right)}{1-\cos\left(\frac{2\pi}{p-1}(\frac{\alpha_j}{2} - \frac{\alpha_s}{2})\right)} \leq K_p \cdot (L_s(2x_r))^2 \leq \frac{34^p K_p}{16p^2}.$$

Combining (2.36) and the slightly simpler estimate

$$\left\|\left(\boldsymbol{L}^A\right)^{-1}\right\|_{\mathrm{F}}^2 = \sum_{r=0}^{p-1}\sum_{s=0}^{p-1} |l_s^{AS}(x_r^P)|^2 \leq \frac{34^p K_p}{16},$$

the assertion follows by bounding the spectral norm by the Frobenius norm. Setting $x = \frac{2\pi}{p-1}$ in Lemma 2.1 (2.6) finally yields $K_p\sqrt{34} \leq 6^2$. ∎

3. Butterfly scheme. As pointed out in the introduction, we aim to compute

$$u_j = u(\boldsymbol{x}_j) = \sum_{k=1}^{M_2} \hat{u}_k \mathrm{e}^{2\pi\mathrm{i}\boldsymbol{\xi}_k \boldsymbol{x}_j/N}, \quad j = 1,\ldots,M_1, \tag{3.1}$$

for a space dimension $d \in \mathbb{N}$, a nonharmonic bandwidth $N = 2^L$, $L \in \mathbb{N}$, a set of frequencies $\widetilde{T} = \{\boldsymbol{\xi}_k \in [0, N]^d : k = 1, \ldots, M_2\}$, a set of Fourier coefficients $\hat{u}_k \in \mathbb{C}$, $k = 1, \ldots, M_2$, and a set of evaluation nodes $\widetilde{X} = \{\boldsymbol{x}_j \in [0, N]^d : j = 1, \ldots, M_1\}$. For $d = 1$ and no restrictions on the sampling sets $\widetilde{T}$ and $\widetilde{X}$, the following considerations just give a slightly more expensive variant of the FFT for nonequispaced data in space and frequency domain [6, 9], but we include this case for notational convenience. In case $d \geq 2$, $M_1 = M_2 = N^{d-1}$, and well distributed sampling sets on smooth $d-1$ dimensional manifolds, the following dyadic decompositions of the sampling sets remain sparse. The butterfly graph, which represents the admissible pairs where computations are performed, remains sparse as well and a favourable complexity can be achieved.

In the one dimensional case, we consider $T := X := [0, N]$ and the dyadic decomposition

$$\begin{aligned} X_{l,m} &:= \big[N/2^l m, N/2^l (m+1)\big) && \text{for } m = 0, \ldots, 2^l - 1, \\ T_{L-l,n} &:= \big[N/2^{L-l} n, N/2^{L-l} (n+1)\big) && \text{for } n = 0, \ldots, 2^{L-l} - 1, \end{aligned}$$

for $l = 0, \ldots, L$, where the level in the butterfly scheme and locations are denoted by l and m, n, respectively. Moreover note that we always include the point N in the rightmost sets $X_{l,2^l-1}$ and $T_{l,2^l-1}$, $l = 0, \ldots, L$. The decomposition of the interval $X = [0, N]$ is illustrated in Figure 3.1, all in the sense of Theorem 2.6 admissible pairs $(X_{l,m}, T_{L-l,n})$ are shown in Figure 3.2.

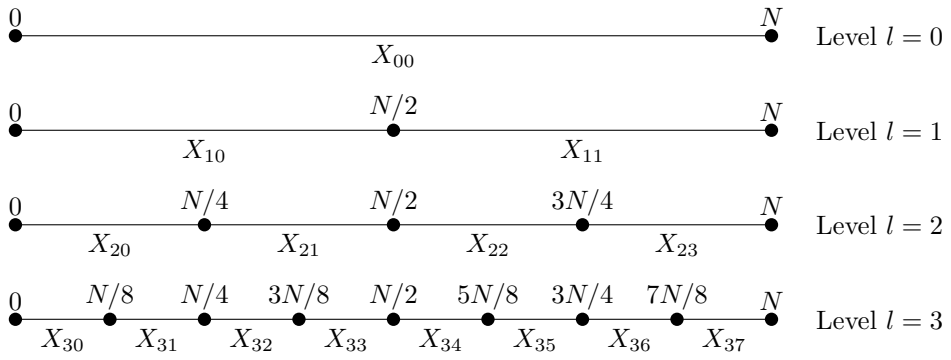

FIGURE 3.1. *Dyadic decomposition of X.*

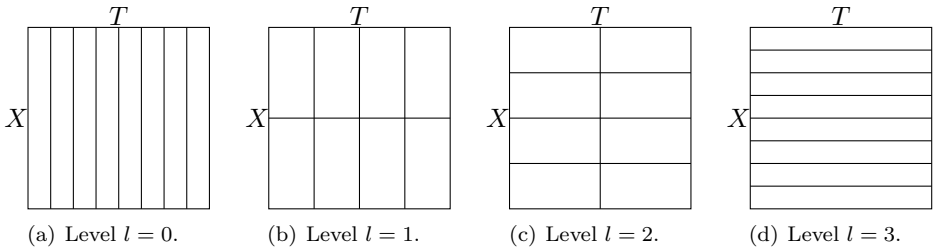

(a) Level $l = 0$. (b) Level $l = 1$. (c) Level $l = 2$. (d) Level $l = 3$.

FIGURE 3.2. *Admissible pairs of $X = T = [0, 8]$.*

If we represent all intervals of the two dyadic decompositions by a node in a graph

and have edges for inclusions, we obtain two binary trees. Furthermore, all admissible pairs $(X_{l,m}, T_{L-l,n})$ are nodes in the butterfly graph, they are given as combinations of nodes in the l-th level of the X-tree and the $(L-l)$-th level in the T-tree. An edge is set if and only if the nodes in the X-tree and in the T-tree are connected, see Figure 3.3.

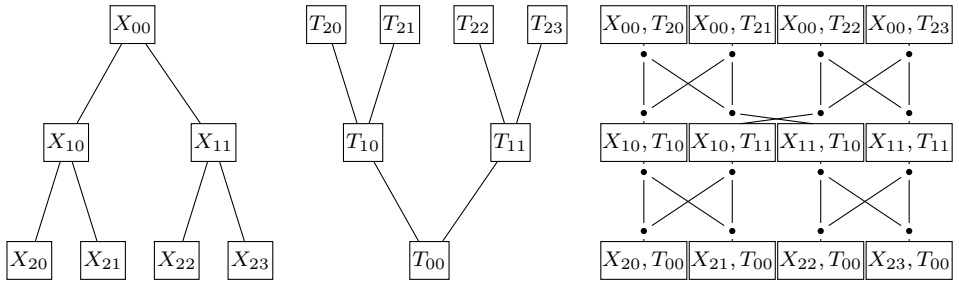

(a) X-tree. (b) T-tree. (c) Butterfly graph.

FIGURE 3.3. *Trees and butterfly graph for $N = 4$.*

For spatial dimension $d \geq 2$, we have $T := X := [0, N]^d$ and decompose dyadically for levels $l = 0, \ldots, L$ into the boxes

$$X_{l,\boldsymbol{m}} := X_{l,m_1} \times \ldots \times X_{l,m_d}, \quad T_{L-l,\boldsymbol{n}} := T_{L-l,n_1} \times \ldots \times T_{L-l,n_d},$$

with the location parameters $\boldsymbol{m} := (m_1, \ldots, m_d)$, $0 \leq m_1, \ldots, m_d \leq 2^l - 1$, and $\boldsymbol{n} := (n_1, \ldots, n_d)$, $0 \leq n_1, \ldots, n_d \leq 2^{L-l} - 1$.

The butterfly scheme in Algorithm 1 now traverses the butterfly graph top down. Starting from level $l = 0$ and local sums over frequencies, we define in each level approximations from its two predecessors. Level by level, they include more frequencies and are valid in smaller spatial boxes. The final approximation is a function piecewise defined in the smallest X-boxes.

3.1. Error analysis. In contrast to other analysis-based fast algorithms, the butterfly scheme uses a sequence of approximations and the local expansion degree depends not only on the target accuracy $\varepsilon > 0$ but also mildly on the nonharmonic bandwidth N. This behaviour is illustrated also numerically in Section 4.2.

THEOREM 3.1. *Let $L \in \mathbb{N}$, $N = 2^L$, $T, X \subset [0, N]^d$, and $p \in \mathbb{N}$, $p \geq 5$, then the approximation* (3.4) *to the function* (3.1) *obeys the error estimate*

$$\|u - \widetilde{u}\|_{C(X)} \leq \frac{(C_p + 1)(C_p^{d(L+1)} - 1)}{C_p - 1} c_p \|\hat{\boldsymbol{u}}\|_1.$$

Proof. Define for all levels $l = 0, \ldots, L$ and the frequency indices $\boldsymbol{n} \in \mathbb{N}_0^d$, $\|\boldsymbol{n}\|_\infty < 2^{L-l}$ the local sums

$$u^{T_{L-l,\boldsymbol{n}}} := \sum_{\boldsymbol{\xi}_k \in T_{L-l,\boldsymbol{n}} \cap \widetilde{T}} \hat{u}_k \mathrm{e}^{2\pi \mathrm{i} \boldsymbol{\xi}_k \cdot \boldsymbol{x}/N}$$

and for the spatial indices $\boldsymbol{m} \in \mathbb{N}_0^d$, $\|\boldsymbol{m}\|_\infty < 2^l$, the error term

$$E_{l,\boldsymbol{m}} := \sum_{\boldsymbol{n} \in \mathbb{N}_0^d; \|\boldsymbol{n}\|_\infty < 2^{L-l}} \|u^{T_{L-l,\boldsymbol{n}}} - u^{X_{l,\boldsymbol{m}} T_{L-l,\boldsymbol{n}}}\|_{C(X_{l,\boldsymbol{m}})},$$

Algorithm 1 Butterfly scheme.

Input: $d, L, M_1, M_2, p \in \mathbb{N}$, $p \geq 2$, $N = 2^L$,
$\hat{u}_k \in \mathbb{C}$, $\boldsymbol{\xi}_k \in [0, N]^d$, $k = 1, \ldots, M_2$,
$\boldsymbol{x}_j \in [0, N]^d$, $j = 1, \ldots, M_1$.

for $n_1, \ldots, n_d = 0, \ldots, 2^L - 1$ ***do***

$$u^{T_{L,\boldsymbol{n}}}(\boldsymbol{x}) := \sum_{\boldsymbol{\xi}_k \in T_{L,\boldsymbol{n}} \cap \widetilde{T}} \hat{u}_k \mathrm{e}^{2\pi \mathrm{i} \boldsymbol{\xi}_k \cdot \boldsymbol{x}/N} \tag{3.2}$$
$$u^{X_{0,\mathbf{0}} T_{L,\boldsymbol{n}}} := \mathcal{J}_p^{X_{0,\mathbf{0}} T_{L,\boldsymbol{n}}} u^{T_{L,\boldsymbol{n}}}$$

end for

for $l = 1, \ldots, L$ ***do***
for $m_1, \ldots, m_d = 0, \ldots, 2^l - 1$ and $n_1, \ldots, n_d = 0, \ldots, 2^{L-l} - 1$ ***do***

$$u^{X_{l,\boldsymbol{m}} T_{L-l,\boldsymbol{n}}} := \mathcal{J}_p^{X_{l,\boldsymbol{m}} T_{L-l,\boldsymbol{n}}} \sum_{\boldsymbol{k} \in \{0,1\}^d} u^{X_{l-1,\lfloor \boldsymbol{m}/2 \rfloor} T_{L-l+1, 2\boldsymbol{n}+\boldsymbol{k}}} \tag{3.3}$$

end for
end for
for $j = 1, \ldots, M_1$ ***do***

$$\boldsymbol{m} := \lfloor \boldsymbol{x}_j \rfloor$$
$$\widetilde{u}(\boldsymbol{x}_j) := u^{X_{L,\boldsymbol{m}} T_{0,\mathbf{0}}}(\boldsymbol{x}_j) \tag{3.4}$$

end for

Output: Approximate function values $\widetilde{u}(\boldsymbol{x}_j)$, $j = 1, \ldots, M_1$.

which by definition fulfils $\|u - \widetilde{u}\|_{C(X)} = \max_{\boldsymbol{m} \in \mathbb{N}_0^d, \|\boldsymbol{m}\|_\infty < 2^L} E_{L,\boldsymbol{m}}$. Using Theorem 2.6 and the triangle inequality, this quantity can be bounded for the zeroth level by

$$\begin{aligned} E_{0,\mathbf{0}} &= \sum_{\boldsymbol{n} \in \mathbb{N}_0^d; \|\boldsymbol{n}\|_\infty < 2^L} \|u^{T_{L,\boldsymbol{n}}} - \mathcal{J}_p^{X_{0,\mathbf{0}} T_{L,\boldsymbol{n}}} u^{T_{L,\boldsymbol{n}}}\|_{C(X_{0,\mathbf{0}})} \\ &\leq \frac{(1 + C_p)(C_p^d - 1)}{C_p - 1} c_p \sum_{\boldsymbol{n} \in \mathbb{N}_0^d; \|\boldsymbol{n}\|_\infty < 2^L} \sum_{\boldsymbol{\xi}_k \in T_{L,\boldsymbol{n}} \cap \widetilde{T}} |\hat{u}_k| \\ &\leq \frac{(1 + C_p)(C_p^d - 1)}{C_p - 1} c_p \|\hat{\boldsymbol{u}}\|_1. \end{aligned}$$

For $l > 0$, adding and subtracting the term $\mathcal{J}_p^{X_{l,\boldsymbol{m}} T_{L-l,\boldsymbol{n}}} u^{T_{L-l,\boldsymbol{n}}}$ yields

$$\begin{aligned} E_{l,\boldsymbol{m}} = \sum_{\substack{\boldsymbol{n} \in \mathbb{N}_0^d \\ \|\boldsymbol{n}\|_\infty < 2^{L-l}}} &\|u^{T_{L-l,\boldsymbol{n}}} - \mathcal{J}_p^{X_{l,\boldsymbol{m}} T_{L-l,\boldsymbol{n}}} u^{T_{L-l,\boldsymbol{n}}} \\ &+ \mathcal{J}_p^{X_{l,\boldsymbol{m}} T_{L-l,\boldsymbol{n}}} u^{T_{L-l,\boldsymbol{n}}} - u^{X_{l,\boldsymbol{m}} T_{L-l,\boldsymbol{n}}} \|_{C(X_{l,\boldsymbol{m}})}. \end{aligned}$$

Using the triangle inequality, the first norm can be bounded as for the zeroth level, and we proceed by applying equation (3.3), factoring out the interpolation operator, using the dyadic decomposition $T_{L-l,\boldsymbol{n}} = \cup_{\boldsymbol{k}\in\{0,1\}^d} T_{L-l+1,2\boldsymbol{n}+\boldsymbol{k}}$, and the relation $X_{l,\boldsymbol{m}} \subset X_{l-1,\lfloor \boldsymbol{m}/2 \rfloor}$ to obtain

$$\begin{aligned}
&\sum_{\substack{\boldsymbol{n}\in\mathbb{N}_0^d \\ \|\boldsymbol{n}\|_\infty < 2^{L-l}}} \|\mathcal{J}_p^{X_{l,\boldsymbol{m}}T_{L-l,\boldsymbol{n}}} u^{T_{L-l,\boldsymbol{n}}} - u^{X_{l,\boldsymbol{m}}T_{L-l,\boldsymbol{n}}}\|_{C(X_{l,\boldsymbol{m}})} \\
&\le \sum_{\substack{\boldsymbol{n}\in\mathbb{N}_0^d \\ \|\boldsymbol{n}\|_\infty < 2^{L-l}}} \left\|\mathcal{J}_p^{X_{l,\boldsymbol{m}}T_{L-l,\boldsymbol{n}}}\right\| \sum_{\boldsymbol{k}\in\{0,1\}^d} \left\|u^{T_{L-l+1,2\boldsymbol{n}+\boldsymbol{k}}} - u^{X_{l-1,\lfloor \boldsymbol{m}/2\rfloor}T_{L-l+1,2\boldsymbol{n}+\boldsymbol{k}}}\right\|_{C(X_{l-1,\lfloor \frac{\boldsymbol{m}}{2}\rfloor})} \\
&\le C_p^d E_{l-1,\lfloor \frac{\boldsymbol{m}}{2}\rfloor}.
\end{aligned}$$

Hence, we inductively find for $\boldsymbol{m} \in \mathbb{N}_0^d$, $\|\boldsymbol{m}\|_\infty < 2^L$, the relation

$$\begin{aligned}
E_{L,\boldsymbol{m}} &\le \frac{(1+C_p)(C_p^d-1)}{C_p-1} c_p \|\hat{\boldsymbol{u}}\|_1 + C_p^d E_{L-1,\lfloor \frac{\boldsymbol{m}}{2}\rfloor} \\
&\le \frac{(1+C_p)(C_p^d-1)}{C_p-1} c_p \cdot \frac{C_p^{d(L+1)}-1}{C_p^d-1} \|\hat{\boldsymbol{f}}\|_1,
\end{aligned}$$

which proves the assertion. □

COROLLARY 3.2. *Under the assumptions of Theorem 3.1, let for given $\varepsilon \in (0,1]$ the expansion degree $p \in \mathbb{N}$ fulfil*

$$p \ge \max\{10, 2|\log\varepsilon|, 2d(L+1)\},$$

then $\|u - \widetilde{u}\|_{C(X)} \le \varepsilon \|\hat{\boldsymbol{u}}\|_1$.

Proof. Direct calculation shows for $p \ge 10$ the relation

$$p \ge 1 + \pi\sqrt{\mathrm{e}C_p}.$$

Together with $p \ge 2d(L+1)$ this yields

$$\log\frac{p-1}{\pi} - \frac{d(L+1)}{p}\log C_p \ge \frac{1}{2}$$

and multiplication by $p \ge 2|\log\varepsilon|$ finally gives the bound

$$C_p^{d(L+1)} \left(\frac{\pi}{p-1}\right)^p \le \varepsilon$$

from which the assertion follows by Theorem 3.1. □

3.2. Computational complexity. Again, we start with the univariate case $d = 1$. For the level $l = 0$, the local sums $u^{T_{L,n}}$ in (3.2) are evaluated at Chebychev nodes x_r^X, $r = 0, \dots, p-1$, and this takes $\mathcal{O}(pM_2)$ floating point operations. For each level $l = 0, \dots, L$, we have to apply the interpolation operator $N = 2^L$ times and a single application takes $\mathcal{O}(p^2)$ floating point operations, cf. Section 2.3.3. Finally, we evaluate the function $\widetilde{u}(x_j)$ at all sampling nodes, which takes $\mathcal{O}(pM_1)$ floating point operations for the original approach [17] and the approach in Section 2.3.2 with precomputation of the Lagrange functions at the evaluation nodes. Without such precomputations, a straightforward evaluation of the Lagrange functions leads to $\mathcal{O}(p^2M_1)$

floating point operations for this step. Assuming $M_1, M_2 = \mathcal{O}(N)$ and a target accuracy $\varepsilon > 0$, this sums up to the total computational costs $\mathcal{O}(N \log N(|\log \varepsilon| + \log N)^2)$.

Generalising to $d \geq 2$, we assume that the sets $\widetilde{T}, \widetilde{X} \subset [0, N]^d$ and their dyadic subdivisions are sparse in the sense

$$|\{\boldsymbol{m} \in \mathbb{N}_0^d : m_1, \dots, m_d \leq 2^l - 1,\ \widetilde{X} \cap X_{l,\boldsymbol{m}} \neq \emptyset\}| \leq C 2^{(d-1)l},$$
$$|\{\boldsymbol{n} \in \mathbb{N}_0^d : n_1, \dots, n_d \leq 2^{L-l} - 1,\ \widetilde{T} \cap T_{L-l,\boldsymbol{m}} \neq \emptyset\}| \leq C 2^{(d-1)(L-l)}$$

for some absolute constant $C \in \mathbb{R}$. In particular, $M_1 = |\widetilde{X}|$ and $M_2 = |\widetilde{T}|$ fulfil $M_1, M_2 = \mathcal{O}(N^{d-1})$ and the above condition is satisfied if the sets lie on some smooth $(d-1)$-dimensional manifold in $[0, N]^d$, see also Figure [17, Fig. 5]. Under this sparsity assumption, the number of admissible pairs on which we need to compute is $\mathcal{O}(N^{d-1})$ in each level of the butterfly scheme and a single application of the interpolation operator takes $\mathcal{O}(p^{d+1})$ floating point operations. Finally, the evaluation of the function $\widetilde{u}(\boldsymbol{x}_j)$ at all sampling nodes takes $\mathcal{O}(p^d M_1)$ floating point operations in all approaches, in case of on-the-fly evaluation of the Lagrange functions in tensor product form the costs are amortized. In total, this sums up to computational costs $\mathcal{O}(N \log N(|\log \varepsilon| + \log N)^{d+1})$. The exponent $d+1$ of the last term can be decreased to d by using $\log c_p \leq -Cp \log p$ and the techniques in [7]. A similar improvement might be possible by reducing the p^d dimensional ansatz to one which lives on the $d-1$ dimensional manifold.

4. Numerical experiments. The implementation of the butterfly sparse FFT is realised in MATLAB 7.10.0 (R2010a) for the dimensions $d = 1, 2, 3, 4$. We use one node of a Dell PowerEdge R900, 96GByte, 2.4GHz Intel Xeon 7450, CentOS5.5, for all numerical experiments.

4.1. Local accuracy and stability. The first two experiments are dedicated to the approximation in one pair of admissible boxes. Let the nonharmonic bandwidth $N = 2^L$, $L = 10, 14$, the level $l = 5$, and the boxes $A = [0, 2^l]$, $B = [0, 2^{L-l}]$ be given. Draw nodes $x_j \in A$, $j = 1, \dots, M_1$, $M_1 = N$, and $\xi_k \in B$, $k = 1, \dots, M_2$, $M_2 = N$, at random from the uniform distribution and define the Fourier matrix

$$\boldsymbol{F} := \left(\mathrm{e}^{2\pi \mathrm{i} \xi_k \cdot x_j / N}\right)_{j=1,k=1}^{M_1,M_2}.$$

This matrix is approximately of low rank and we consider the expansions from Sections 2.3.1 and 2.3.2,

$$\widetilde{\boldsymbol{F}} := \boldsymbol{F}^A (\boldsymbol{M}^{AB})^{-1} \boldsymbol{F}^B \quad \text{or} \quad \widetilde{\boldsymbol{F}} := \widetilde{\boldsymbol{L}}^A \boldsymbol{F}^B$$

with the auxiliary matrices

$$\boldsymbol{F}^A := \left(\mathrm{e}^{2\pi \mathrm{i} \xi_s^B x_j / N}\right)_{j=1,s=0}^{M_1,p-1}, \quad \boldsymbol{F}^B := \left(\mathrm{e}^{2\pi \mathrm{i} \xi_k x_r^A / N}\right)_{r=0,k=1}^{p-1,M_2},$$
$$\widetilde{\boldsymbol{L}}^A := \left(\mathrm{e}^{2\pi \mathrm{i}\left(c^B + \frac{w^B}{2}\right) x_j / N} l_r^{AB}(x_j) \mathrm{e}^{-2\pi \mathrm{i}\left(c^B + \frac{w^B}{2}\right) x_r^A / N}\right)_{j=1,r=0}^{M_1,p-1},$$

respectively. In both cases, Theorem 2.6 assures

$$\varepsilon_1 := \max_{\substack{\hat{\boldsymbol{f}} \in \mathbb{C}^{M_2} \\ \|\hat{\boldsymbol{f}}\|_1 = 1}} \left\| \boldsymbol{F}\hat{\boldsymbol{f}} - \widetilde{\boldsymbol{F}}\hat{\boldsymbol{f}} \right\|_\infty = \max_{\substack{j=1,\dots,M_1 \\ k=1,\dots,M_2}} \left| \boldsymbol{F}_{j,k} - \widetilde{\boldsymbol{F}}_{j,k} \right| \leq c_p = \frac{1}{\pi p} \left(\frac{\pi}{p-1}\right)^p.$$

We compare the quantity ε_1 for both realisations and for the original approach [17] in Figure 4.1. The original scheme differs from the variant in Section 2.3.1 in the choice of interpolation nodes in $x_r^A \in A$, where we use zeros of Chebychev polynomials instead of extrema, and in the choice of the 'equivalent sources' $\xi_s^B \in B$, where we use equidistant points instead of Chebyshev extrema. In all three cases, the error decays exponentially with increasing expansion degree p, as predicted by Theorem 2.6 for the equidistant points $\xi_s^B \in B$. However note that both monomial type approaches achieve only an accuracy $\varepsilon_1 \approx 10^{-8}$ and suffer from severe instabilities for values $p \geq 9$ which is well predicted by the quantity $\kappa(\boldsymbol{M}^{AB})\mu$, where $\mu \approx 2 \cdot 10^{-16}$ denotes the machine precision and κ the spectral condition number.

The second experiment analyses the stability of the monomial and the Lagrange type approaches as theoretically discussed in Section 2.4. Figure 4.2 shows the growth of the condition numbers of the matrices $\boldsymbol{M}^{AB}$, $\boldsymbol{L}^A \in \mathbb{C}^{p\times p}$, and lower and upper bounds, cf. Theorems 2.7 and 2.8.

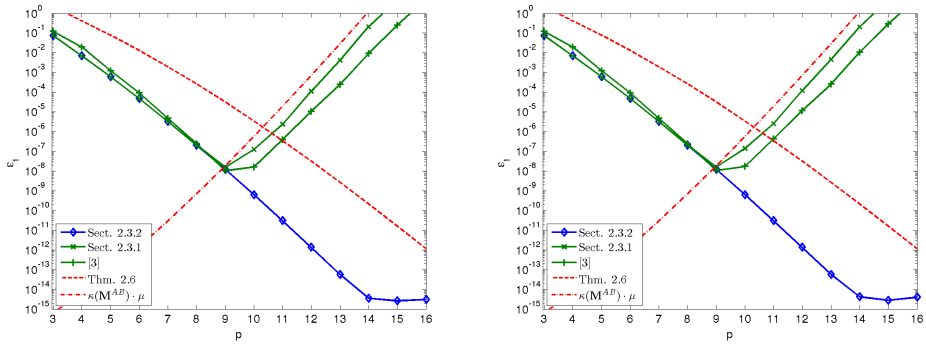

(a) $N = 2^{10}$ and $l = 5$.

(b) $N = 2^{14}$ and $l = 5$.

FIGURE 4.1. *Relative error ε_1 with respect to the local expansion degree p for the realisation via Lagrange functions, cf. Section 2.3.2, and monomials, cf. Section 2.3.1 and [17].*

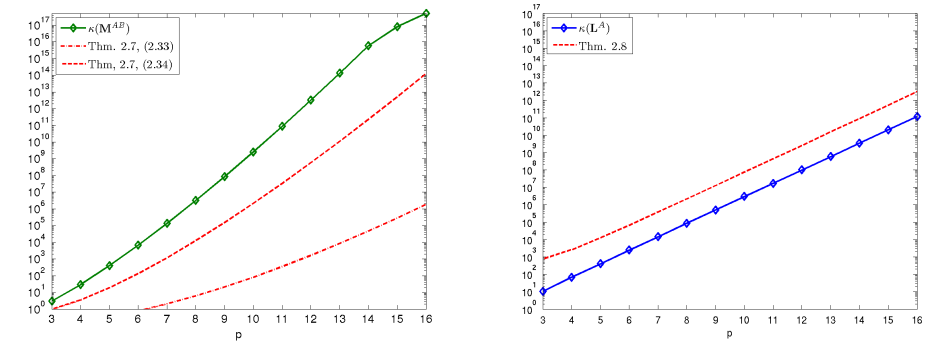

(a) $\kappa(\boldsymbol{M}^{AB})$ and lower bounds.

(b) $\kappa(\boldsymbol{L}^A)$ and upper bounds

FIGURE 4.2. *Condition number of the Vandermonde matrix $\boldsymbol{M}^{AB} \in \mathbb{C}^{p\times p}$, cf. Section 2.3.1 and [17], and the Lagrange matrix $\boldsymbol{L}^A \in \mathbb{C}^{p\times p}$, cf. Section 2.3.2, with respect to the local expansion degree p.*

4.2. Accuracy of the Butterfly scheme. Regarding the accuracy of the whole algorithm, we draw coefficients $\hat{u}_k \in [-\frac{1}{2}, \frac{1}{2}] \times [-\frac{1}{2}, \frac{1}{2}]\mathrm{i}$, $k = 1, \ldots, M_2$, at random from the uniform distribution and consider the relative error

$$\varepsilon_2 := \max_{j=1,\ldots,M_1} \frac{|u(\boldsymbol{x}_j) - \widetilde{u}(\boldsymbol{x}_j)|}{\|\hat{\boldsymbol{u}}\|_1} \leq \frac{(C_p + 1)(C_p^{d(L+1)} - 1)}{C_p - 1} c_p,$$

where $u, \widetilde{u} : [0, N]^d \to \mathbb{C}$ denote the function to evaluate (3.1) and its approximation (3.4). We compare the quantity ε_2 and the upper bound from Theorem 3.1 for the monomial and the Lagrange type realisation in Figure 4.3 (top). In these two tests as well as further experiments for $d = 2$, $d = 3$, and $d = 4$, the total error decays exponentially with p but is again limited for the monomial type realisation. In all cases, a least squares fit reveals a numerical error decay $\varepsilon_2 \approx C \cdot 16^{-p}$, where the constant C seems to depend neither on d nor L.

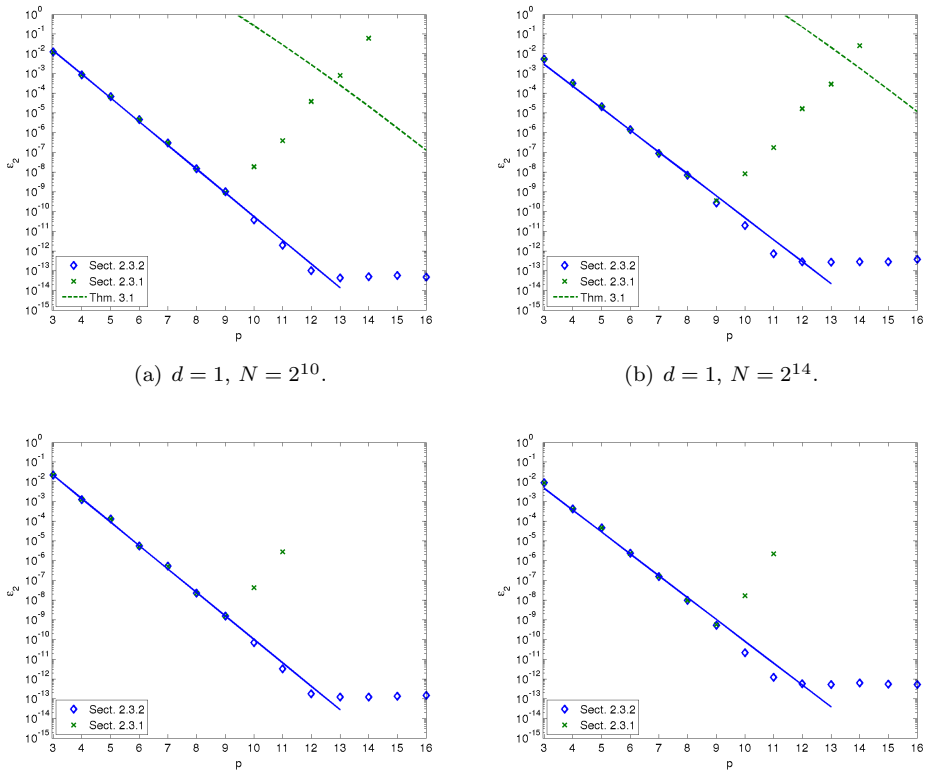

(a) $d = 1$, $N = 2^{10}$. (b) $d = 1$, $N = 2^{14}$.

(c) $d = 2$, $N = 2^{10}$. (d) $d = 2$, $N = 2^{14}$.

FIGURE 4.3. *Relative error ε_2 with respect to the local expansion degree p for the realisation via Lagrange functions, cf. Section 2.3.2, and monomials, cf. Section 2.3.1.*

Our second experiment touches the question whether the error really increases for increasing nonharmonic bandwidth as predicted by Corollary 3.2, i.e., $\varepsilon_2 \approx C_{p,d} N$. While randomly drawn coefficients $\hat{u}_k \in \mathbb{C}$, as in the previous test, did not show this increase, using constant coefficients $\hat{u}_k = 1$ support a weak increase $\varepsilon_2 \approx C_{p,d} L = C_{p,d} \log_2 N$, cf. in Figure 4.4.

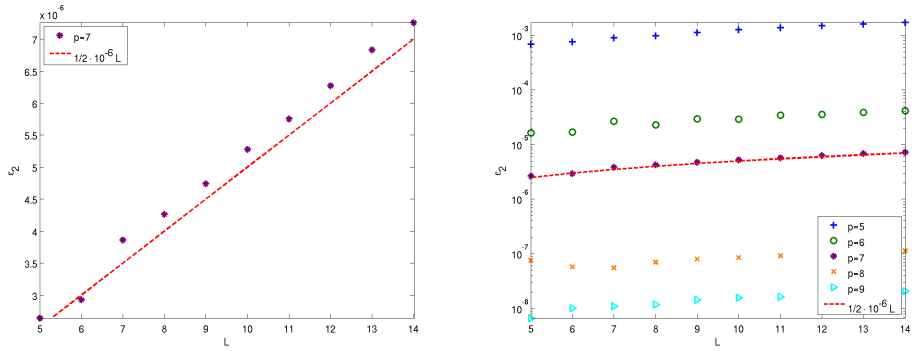

(a) $d = 1$, $\hat{u}_k = 1$ (b) Logarithmic scale.

FIGURE 4.4. *Relative error ε_2 with respect to the nonharmonic bandwidth L.*

4.3. Computational times. Finally, we compare the computational times, measured by the MATLAB functions `tic` and `toc`, of the naive evaluation (1.1) and Algorithm 1 for fixed spatial dimensions $d = 1, 2, 3, 4$, fixed local expansion degrees $p = 4, 8$, and with respect to increasing nonharmonic bandwidth N. We draw coefficients $\hat{u}_k \in [-\frac{1}{2}, \frac{1}{2}] \times [-\frac{1}{2}, \frac{1}{2}]$i and source and target nodes $\boldsymbol{\xi}_k, \boldsymbol{x}_j \in [0, N]^d$, $k = 1, \dots, M_2$, $j = 1, \dots, M_1$, at random from the uniform distribution (on the submanifold). As discussed in Section 3.2, we consider three realisations of the interpolation operator, the monomial type basis, cf. Section 2.3.1, the Lagrange type basis, cf. Section 2.3.2, and the Lagrange type basis with precomputation of the Lagrange functions at the final evaluation nodes, denoted subsequently by Section 2.3.2*.

Figure 4.5 shows the measured times for $d = 1$ and $M_1 = M_2 = N$ sampling nodes in $\boldsymbol{\xi}_k, \boldsymbol{x}_j \in [0, N]$. The break even with the naive method occurs at $N = 32$ and we see some increase for a larger local expansion degree $p = 8$ when no precomputation is done. Figure 4.6 gives the results for $d = 2, 3, 4$ with $M_1 = M_2 = N^{d-1}$ sampling nodes on ellipses, spheres, and hyperplanes, respectively. Precomputation of the Lagrange functions in the last step of the algorithm does not gain any improvement here. Finally note that the break even with the naive algorithm occurs at a suitable problem size but a further reduction in absolute computing time is necessary for real applications.

5. Summary. Recently, the butterfly approximation scheme has been used for the development of a fast Fourier transform for sparse data [1, 17] which takes $\mathcal{O}(N^{d-1} \log N p^{d+1})$ floating point operations for $d \geq 2$, $M_1 = M_2 = \mathcal{O}(N^{d-1})$, and well distributed sampling sets $\widetilde{T}, \widetilde{X}$ on smooth $d-1$ dimensional manifolds, and a local expansion degree $p \in \mathbb{N}$.

We presented a rigorous error analysis of this algorithm, showing that the local expansion degree grows at most like $p \approx |\log \varepsilon| + \log N$ and thus gave a complexity estimate for the scheme. Moreover, we showed theoretically as well as numerically, that the original scheme becomes numerically unstable if a large local expansion degree is used and developed a stable variant by representing all approximations in a Lagrange type basis.

Acknowledgement. The authors thank the referees for their valuable suggestions and gratefully acknowledge support by the German Research Foundation within

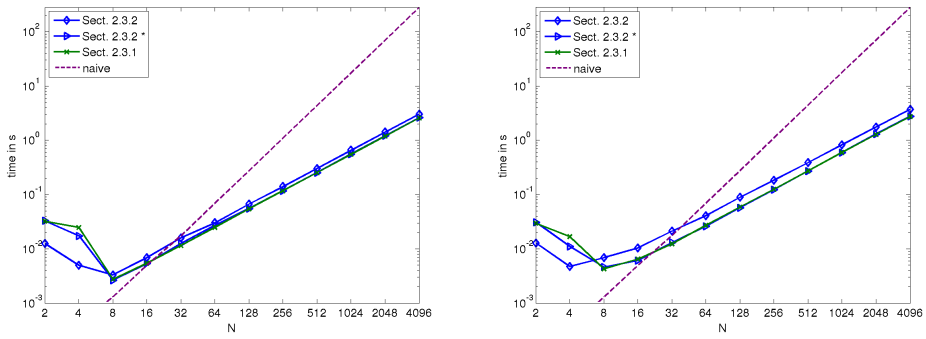

(a) $d = 1$, $p = 4$. (b) $d = 1$, $p = 8$.

FIGURE 4.5. *Computational time of the butterfly (nonsparse) FFT with respect to the nonharmonic bandwidth and problem size* $N = M_1 = M_2$.

the project KU 2557/1-2 and by the Helmholtz Association within the young investigator group VH-NG-526.

REFERENCES

[1] A. A. Aydıner, W. C. Chew, J. Song, and T. J. Cui. A sparse data fast Fourier transform (SDFFT). *IEEE Trans. Antennas and Propagation*, 51(11):3161–3170, 2003.

[2] E. Candès, L. Demanet, and L. Ying. A fast butterfly algorithm for the computation of Fourier integral operators. *Multiscale Model. Simul.*, 7(4):1727–1750, 2009.

[3] L. Demanet, M. Ferrara, N. Maxwell, J. Poulson, and L. Ying. A butterfly algorithm for synthetic aperture radar imaging. *SIAM J. Imaging Sci.*, 5(1):203–243, 2012.

[4] P. Duhamel and M. Vetterli. Fast Fourier transforms: a tutorial review and a state of the art. *Signal Process.*, 19(4):259–299, 1990.

[5] A. Edelman, P. McCorquodale, and S. Toledo. The future fast Fourier transform? *SIAM J. Sci. Comput.*, 20(3):1094–1114, 1999.

[6] B. Elbel and G. Steidl. Fast Fourier transform for nonequispaced data. In C. K. Chui and L. L. Schumaker, editors, *Approximation Theory IX*, pages 39 – 46, Nashville, 1998. Vanderbilt University Press.

[7] T. Finck, G. Heinig, and K. Rost. An inversion formula and fast algorithms for Cauchy-Vandermonde matrices. *Linear Algebra Appl.*, 183:179–191, 1993.

[8] M. Frigo and S. G. Johnson. The design and implementation of FFTW3. *Proceedings of the* IEEE, 93(2):216 – 231, 2005.

[9] L. Greengard and J.-Y. Lee. Accelerating the nonuniform fast Fourier transform. *SIAM Rev.*, 46(3):443–454 (electronic), 2004.

[10] J. Keiner, S. Kunis, and D. Potts. Using NFFT 3—a software library for various nonequispaced fast Fourier transforms. *ACM Trans. Math. Software*, 36(4):Art. 19, 30, 2009.

[11] T. G. Kolda and B. W. Bader. Tensor decompositions and applications. *SIAM Rev.*, 51(3):455–500, 2009.

[12] E. Michielssen and A. Boag. A multilevel matrix decomposition algorithm for analyzing scattering from large structures. *IEEE Trans. Antennas and Propagation*, 44(8):1086 –1093, 1996.

[13] M. O'Neil, F. Woolfe, and V. Rokhlin. An algorithm for the rapid evaluation of special function transforms. *Appl. Comput. Harmon. Anal.*, 28(2):203–226, 2010.

[14] T. J. Rivlin. *Chebyshev polynomials*. Pure and Applied Mathematics (New York). John Wiley & Sons Inc., New York, second edition, 1990. From approximation theory to algebra and number theory.

[15] L. N. Trefethen and J. A. C. Weideman. Two results on polynomial interpolation in equally spaced points. *J. Approx. Theory*, 65(3):247–260, 1991.

[16] M. Tygert. Fast algorithms for spherical harmonic expansions, III. *J. Comput. Phys.*,

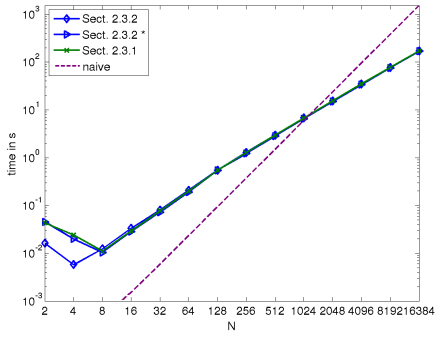

(a) $d = 2$, $p = 4$.

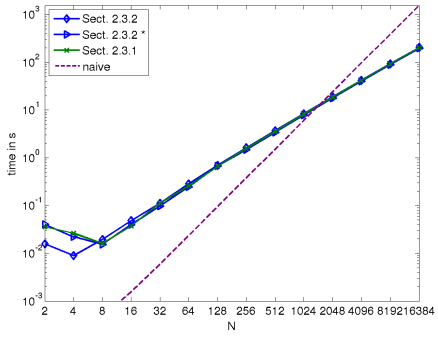

(b) $d = 2$, $p = 8$.

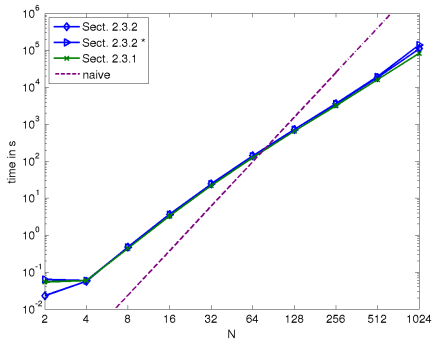

(c) $d = 3$, $p = 4$.

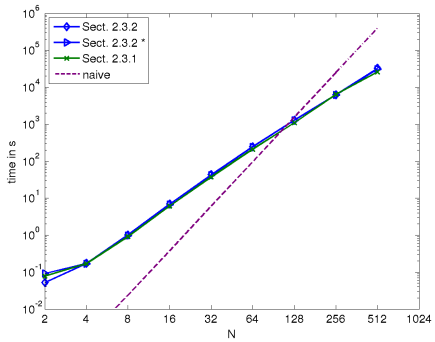

(d) $d = 3$, $p = 8$.

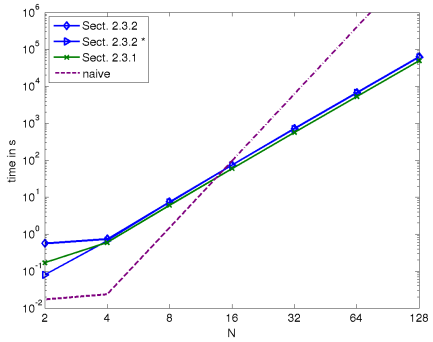

(e) $d = 4$, $p = 4$.

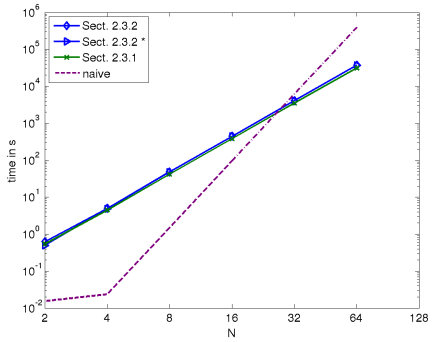

(f) $d = 4$, $p = 8$.

FIGURE 4.6. *Computational time of the butterfly sparse FFT with respect to the nonharmonic bandwidth N and problem sizes $M_1 = M_2 = N^{d-1}$.*

229(18):6181–6192, 2010.

[17] L. Ying. Sparse Fourier transform via butterfly algorithm. *SIAM J. Sci. Comput.*, 31(3):1678–1694, 2009.

[18] L. Ying and S. Fomel. Fast computation of partial Fourier transforms. *Multiscale Model. Simul.*, 8(1):110–124, 2009.